Silicon nanowires-based biosensors for the electrical detection of Escherichia coli

Yousra Benserhir, Anne-Claire Salaün, Florence Geneste, Nolwenn Oliviero, Laurent Pichon, Anne Jolivet-Gougeon

Silicon Nanowires-based biosensors for the electrical detection of *Escherichia coli*

Yousra BENSERHIR[a], Anne-Claire SALAÜN[a,], Florence GENESTE[b], Nolwenn OLIVIERO[c], Laurent PICHON[a] and Anne JOLIVET-GOUGEON[c]*

[a] Univ Rennes, CNRS, IETR [Institut d'Electronique et des Technologies du numéRique] UMR 6164, F-35000 Rennes, France, [b] Univ Rennes, ISCR [Institut des Sciences Chimiques de Rennes] - UMR 6226, F-35000 Rennes, France, [c] Univ Rennes, INSERM, INRAE, Institut NUMECAN [Nutrition Metabolisms and Cancer], F-35000 Rennes, France.

* Corresponding author: asalaun@univ-rennes1.fr

Abstract

One of the main challenges in terms of public health concerns the prevention of bacterial contamination using rapid, highly sensitive and specific detection techniques. The development of highly sensitive bacterial sensors for *Escherichia coli* detection based on networks of silicon nanowires has been carried out in this work. The interest of these nano-objects takes advantage in a large contact surface allowing potentially important interactions with bacteria. Their presence induces a change in electrical interaction through the silicon nanowires array and is the basis for the development of silicon nanowires based electrical resistances acting as bacteria sensors. High specificity of these sensors is ensured by chemical functionalization of the nanowires allowing the binding of specific antibodies targeting the lipopolysaccharide (anti-LPS) of *E. coli*, but not *S. aureus*. The sensor displays a sensitivity of 83 µA per decade of CFU/mL due to the nanometric dimensions of the nanowires. The electrical measurements ensure the detection of various *E. coli* concentrations down to 10^2 CFU/mL. This SiNW biosensor device demonstrated its potential as an alternative tool for real-time bacterial detection as miniaturizable and low-cost integrated electronic sensor compatible with the classical silicon technology.

Keywords

Biosensor; silicon nanowires; *E. coli*; electrical detection; functionalization; antibodies.

1. Introduction

Direct *in situ* detection of pathogenic bacteria in food, water and air is an important public health issue. One of the main challenges concerns the prevention of bacterial contaminations, with effective, rapid, reliable, highly sensitive and specific prevention techniques. Conventional methods for the detection of microorganisms require the use of extraction/amplification/sequencing steps involving long analysis times, thus limiting the implementation of decontamination procedures. They also require complex instruments, and *ex-situ* analysis. An alternative method for bacterial detection is the use of biosensors (Thompson and Deisingh, 2004), which combines a biological recognition mechanism with a physical transduction technique. A number of methods have been demonstrated for bacterial detection, including nanomechanical cantilever sensing (Ndieyira et al., 2008), surface-enhanced Raman spectroscopy (Premasiri et al., 2005), and quartz crystal microbalance-based sensors (Bao et al., 1996). In another way, a high number of biosensors have also been developed for the detection of bacteria, based on electrochemical transduction methods less time-consuming and more sensitive than other techniques such as amperometry, impedance spectroscopy or potentiometry (Ahmed et al., 2014); (Andrade et al., 2015)(Huang et al., 2011)(Kaur et al., 2017)(Benserhir et al., 2022). Another detection method based on electrical measurements has been developed using classical electronics devices (MOSFET, resistors) as sensors (So et al., 2008)(Zhang et al., 2012). More particularly, new emerging technologies based on nano-objects used as sensitive units have been proposed for the development of ultra-high-performance biosensors. For instance, silicon nanowires (SiNWs) open up interesting prospects for the realization of miniaturizable and low-cost biosensors in a fully compatible classical silicon technology, for the real-time analysis of different strains of bacteria with high sensitivity and a low detection limit. The interest of nanowires lies in a large contact surface (high surface/volume ratio) allowing relevant interactions with the

biological object after immobilization, that induces a significant change of the electrical conduction through the network of silicon nanowires. In this case, a very high sensitivity is expected for the sensor under investigation.

Silicon nanowires can be synthesized either by top-down approach (Mikolajick et al., 2013), a technique that requires expensive lithography equipment (electron beam photolithography, deep UV...), or by bottom-up approach (Fasoli and Milne, 2012), based on self-assembly method free of high-cost lithography techniques to pattern nanowires. Advantageously, Vapor-Liquid-Solid (VLS) method (bottom up approach) is compatible with the integration of silicon nanowires in Complementary Metal Oxide Semiconductor (CMOS) technology. In addition, silicon nanowires have also the advantage of being functionalizable, by chemical modification of the silicon surface, allowing a specific antibodies/bacteria binding.

Previous studies demonstrated the interesting capacities of these high-sensitivity sensors based on SiNWs for the detection of low protein concentrations (Cui, 2001)(Kim et al., 2016), gas detection (Chen et al., 2012)(Ni et al., 2013)(Qin et al., 2018)(Yun et al., 2019), detection of DNA strands by nucleic acid hybridization(Cui, 2001)(Midahuen et al., 2022), bacteria (Liao et al., 2019) and SARS-CoV-2 (Gao et al., 2022). Recently, in a previous study carried out by our group, the detection of *Escherichia coli* (*E. coli)* using inter-digitated comb resistors based on non-functionalized silicon nanowires for yes/no diagnosis was demonstrated (Le Borgne et al., 2018). But, in this configuration, the weak point of the sensor was the specific detection and the accurate control of bacterial concentration. In this work, we report new designed inter-digitated comb resistive sensor-based electrodes containing a large number of VLS-interconnected nanowires to increase the sensitivity and with functionalized silicon nanowires for specific detection, acting as proof of concept for linear detection of *E. coli*. The novelty of this work uses an approach that directly detects the contribution of bacteria immobilized on the nanowires with a very low detection level, by optimising the sensitive surface of the sensors in contact with the drop of bacterial suspension, and by

ensuring selectivity by grafting specific antibodies. The fabrication process compatible with CMOS silicon technology, the detection protocol and the performances of the sensor are presented in this work. This study investigates the feasibility of this approach for future applications in the real-time, specific and quantitative detection of *E. coli*.

2. Materials and methods

2.1 Materials

The 3-Aminopropyltriethoxysilane (APTES), Glutaraldehyde (25%) in aqueous solution and Phosphate buffered solution (PBS) with pH 7.4 were purchased from Sigma–Aldrich. The *E. coli* lipopolysaccharide (LPS)-specific antibodies were obtained online from GmbH (Bio-Rad, ABIN2481224), OBT 1844-1 mL (solution 4 mg/mL) and stored at 4 °C. The strains *E. coli* green fluorescent GFP protein-producing (GFP) (ATCC® 25922GFP™) was purchased from the American Type Culture Collection (ATCC) company. The *Staphylococcus aureus* GFP MG 003 was kindly provided by INSERM BMR (https://www.pluginlabs-ouest.fr/en/entity/047d436f-bdb6-4c2f-92f8-7e7fa954831b/arn-regulateurs-bacteriens-et-medecine-brm).

2.2 Fabrication of interdigitated SiNWs electrode arrays

The sensor was a resistor made of inter-digital silicon combs electrodes electrically interconnected by silicon nanowires, made by a two-mask process flow represented in Fig. 1. First, a 300 nm thick layer of N^+ phosphorous *in situ* doped amorphous silicon was deposited on oxidized silicon wafer by Low Pressure Chemical Vapor Deposition (LPCVD) at 550°C and 90 Pa and solid phase crystallized. A first photomask was used to define the electrodes and the interdigital combs (Fig. 1a) by reactive plasma etching of the *in-situ* doped polycrystalline silicon. Then, a second mask was used to deposit 5nm thick gold pads by lift off technique on teeth of doped polycrystalline silicon interdigitated combs electrodes (Fig.1b).

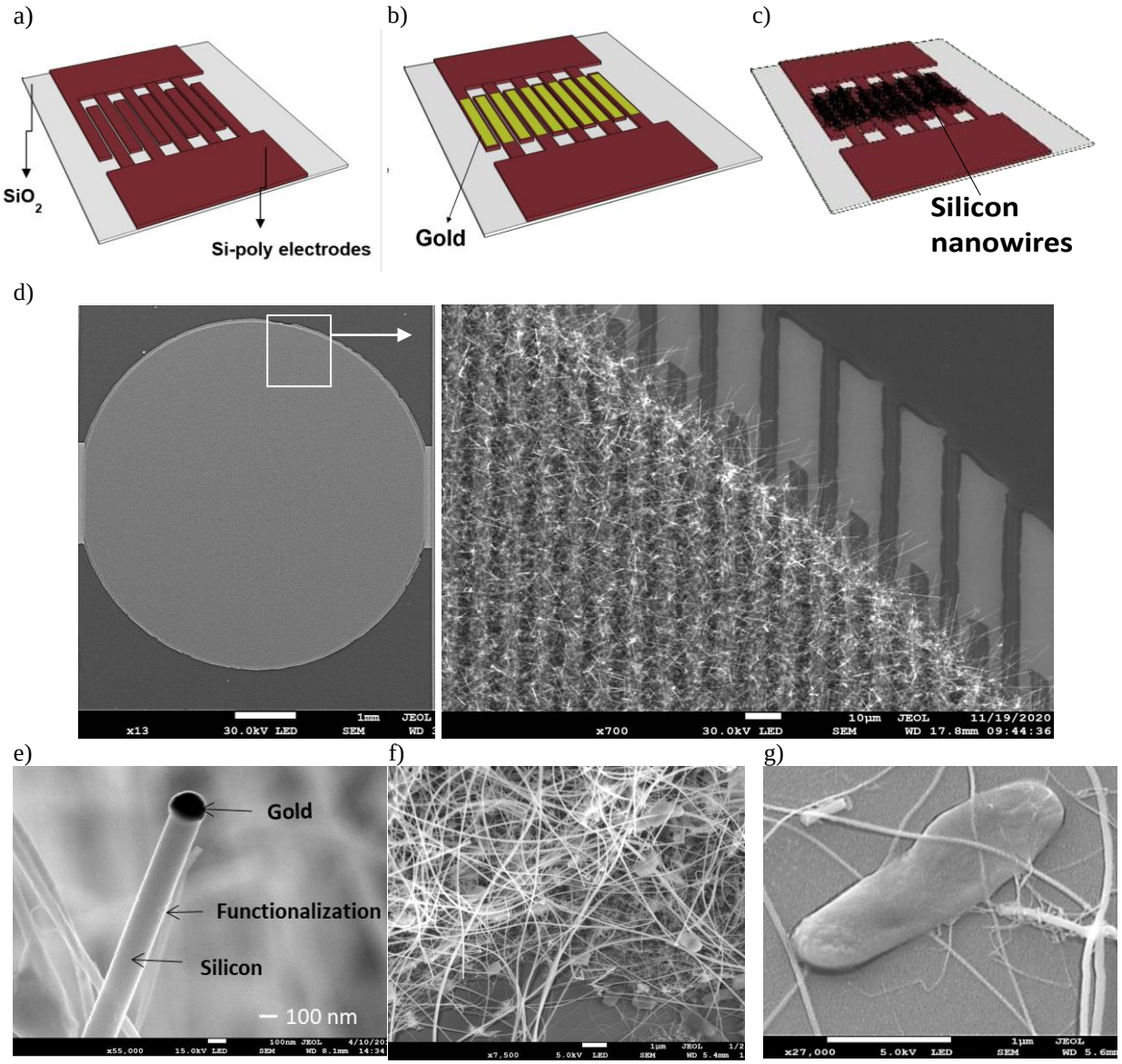

Figure 1: Schematic steps for the fabrication of the bacterial nanosensor: a) definition of interdigitated comb electrodes, b) deposition of a thin layer of gold by lift-off technique, c) formation of silicon nanowires by VLS growth method; SEM image of d) sensor with a zoom on interdigitated comb with nanowires as sensitive units, e) functionalized nanowire (before LPS-antibody deposition), f) zoom on bacteria binding and g) *E. coli* cell showing biological *pili* connecting the silicon nanowires.

The undoped silicon nanowires were then synthesized in LPCVD reactor at 460°C and 40 Pa following the Vapor-Liquid-Solid (VLS) method, using gold as catalyst and silane (SiH_4) as gas precursor (Fig.1c). Dewetting of the gold thin film to form gold droplets takes place during the rise temperature of the reactor, before starting the silane precursor gas injection into the reactor. Interconnection between the nanowires takes place during growth process carried out in vacuum. Thus, native oxide is not formed at the nanowires/nanowires junctions, ensuring electrical connection through nanowire network. Interconnected nanowires ensure electrical contact between the two doped polycrystalline silicon electrodes SiNWs (Pichon et al., 2015). In order to optimise the detection of bacteria, the electrodes were made with a higher number of teeth per unit area than the previous reported structures (Le Borgne et al., 2018), as shown on Scanning Electron Microscopy (SEM) images (Fig. 1d). The glossy surface on the nanowire in Fig.1e represents the functionalization layer. In addition, the electrodes were integrated at the bottom of a resin open micro-chamber moulded by a 3D printing process dedicated to receive the totality of the diluted solution containing the bacteria. This system avoided any phenomenon of dispersion of the bacteria which would not be detected because of the solution spreading. The circular active area of the sensor had a diameter of 6 mm, which included teeth (n=491) of the comb shape electrode, with each tooth spaced by a distance of 3µm.

2.3 Surface functionalization

The samples were first heated at 100°C under vacuum (5 10^{-2} mbar) in a reactor. Then, at room temperature, 2 mL APTES were added under argon in the bottom of the reactor and the samples were left to react with APTES gas for 5 min. The samples were then heated at 100°C under vacuum (5 10^{-2} mbar) for 1h. 1 mL of glutaraldehyde was then added in the bottom of the reactor and the samples were left under glutaraldehyde atmosphere for a specific time. The samples were kept under argon before X-ray photoelectron spectroscopy (XPS) measurement

and antibody attachment.

2.4 Antibody immobilization

The covalent immobilization of anti-*E. coli* LPS antibodies (anti-LPS) was then performed by classical procedures before adding *E. coli* (Fig. 2a). A solution of 10 µL of anti-LPS (Gunda et al., 2014) was deposited on sensors, stored overnight at 4°C in a humid atmosphere. After this step, the wafers were washed with Phosphate-buffered saline (PBS). Finally, milk was used as blocking agent to prevent non-specific binding. The saturation was performed using 10 µL of the milk powder (50g/L in PBS) and the substrate were kept at a temperature of 37°C in a humid atmosphere for 30 min.

2.5 Bacteria binding

A solution was prepared from an overnight culture of the bacterial species (*E. coli or S. aureus).* For bacterial enumeration, serial dilutions were made in sterile distilled water, and then 100µL of each dilution was spread with a sterile plastic rake onto the surface of Columbia agar plates. The number of colonies on each agar plate was achieved after incubation at 37°C for 48 hours. For the tests on sensors, 10µl of each bacterial dilution (10^8, 10^6, 10^4, 10^3 and 10^2 CFU/mL) were deposited at room temperature, to cover the whole active area of the sensors made of nanowires. After 30 min, the sensors were then rinsed 4 times with PBS. A schematic of the modified nanowire with grafted antibody, blocking agent and bacteria immobilization is shown in Fig. 2b.

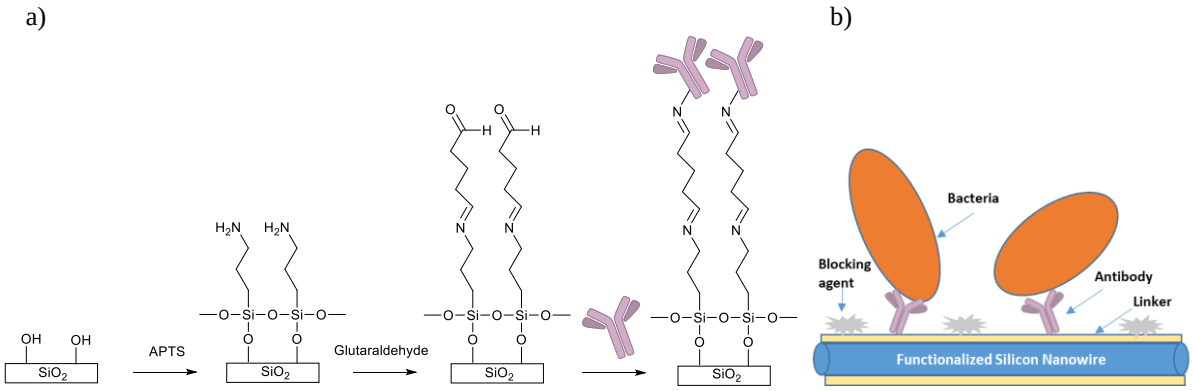

Figure 2: a) Functionalization process with APTES/glutaraldehyde and b) Schematic of the steps: functionalization, immobilization of antibodies, sites saturation with linker and bacteria binding on nanowires.

2.6 X-ray photoelectron spectroscopy (XPS), Fluorescence and Scanning Electron Microscope (SEM) experiments

The XPS analysis was performed with a monochromatic Al KαX-ray source (SPECS XR 50 M and FOCUS 500) at 1486.6 eV with a hemispherical analyser, SPECS Phoibos 150 HR. The analysis chamber was connected to the etching chamber through an ultra-high vacuum chamber to limit surface contamination. The operating pressure in the analysis chamber was 10^{-9} mbar. Spectra were recorded with a pass energy of 14 eV and an energy step of 0.1 eV. Samples were neutralized with an electron flood gun to compensate the charging effect shift. Simulation of the experimental peaks was carried out using a Gaussian-Lorenzian mixed function after background substraction. Fluorescence measurements were performed with a Leica SPE confocal microscope. Green Fluorescent Protein (GFP), excited at 510 nm, was used as biological marker on bacteria for visualizing *E. coli* localization and Fiji software to process and analyse the fluorescence images. SEM observations were performed with a Field emission gun (FEG) JEOL 7600. Sample preparation for SEM imaging requires protocol for preservation of bacteria with several steps: fixation with glutaraldehyde 2.5% for 24 hours followed by dehydration with a graded ethanol series. After fixing and drying, metallization

with a thin layer gold is used to minimize damage and improves topographical contrast.

2.7 Electrical measurements

Detection of bacteria was carried out by electrical measurements of the current-voltage I (V) curve of the resistors used as sensors. Static electrical characteristics of the sensors were collected at room temperature using an Agilent B1500A semiconductor parameter analyzer. Electrical properties of silicon nanowire arrays involved many randomly oriented nanowires. The presence of numerous junctions acting as electrical connexions between the nanowires allowed the current to flow between the interdigitated electrodes. A response reproducibility study was conducted for 14 biosensors made on each wafer and tested in ambient air.

3. Results

3.1 Optimization of the functionalization protocol

To preserve the three-dimensional entangled structure of the Si nanowires, their functionalization was performed by silanization followed by reaction with the well-known cross-linker glutaraldehyde, in vapor phase (Fig. 2a). Indeed, gas phase allowed a good control of the silanization process with the deposition of only 1 or 2 organic layers on the surface (Dauphas et al., 2009). The functionalization steps consisted firstly by (3-Aminopropyl) triethoxysilane (APTES) ($C_9H_{23}NO_3Si$) vapor deposition, the APTES molecule created a chemical bond between silicon atoms with the oxygen of the hydroxyl group on the active layer of SiO_2. Secondly, a glutaraldehyde vapor treatment was then performed. Glutaraldehyde was used as a grafting agent, aldehyde group (COH) creating an imine bond with the amino group (NH_2) of APTES. This immobilization process was first optimized on SiO_2 plane surfaces, before to be applied on SiNWs. The modified surface was analyzed by XPS after treatment with glutaraldehyde gas. The spectra reported in Fig. 3a and 3b clearly

highlighted C1s and N1s XPS peaks. A small C1s peak was observed in the reference spectra corresponding to SiO_2 surfaces, probably due to pollution by oil vapor of the vacuum system during SiO_2 deposition by LPCVD. This peak increased with the reaction time due to the presence of carbon in the organic layer and stabilized after 30 min reaction (Fig. 3c). The deconvolution analysis (Fig. 3a) underlined the presence of four peaks at 282.8, 284.6, 286.7 and 288.9 eV, which could be attributed to C-Si, C-C, C-N and C=O bounds, respectively (Dauphas et al., 2009)(Wang et al., 1995)(Iucci et al., 2010). The last peak at 288.9 eV attested the presence of glutaraldehyde on the surface. The N1s content also increased compared with the reference due to the immobilization of APTES (Fig. 3c). The N1s peak could be deconvoluted into two peaks at 399.6 and 401.9 eV (Fig. 3b), which corresponded to amine nitrogen and to protonated amine, respectively (Carvalho et al., 2016).

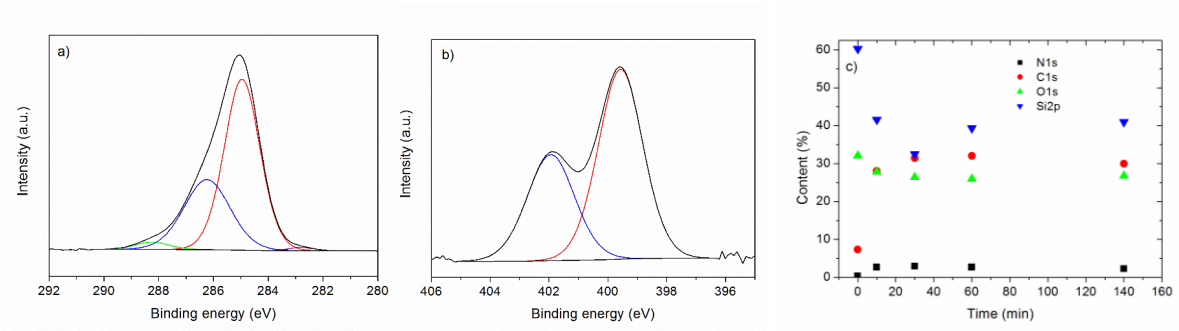

Figure 3: a) C1s, b) N1s photoemission spectra of SiO2 surfaces modified by APTES/glutaraldehyde and c) O1s, Si2p, C1s and N1s content *vs.* reaction time for glutaraldehyde immobilization.

The C1s/N1s ratio calculated, after subtraction of the blank value, which was due to carbon pollution, was estimated around 8 after 10 min and 30 min of glutaraldehyde deposition. This value was consistent with a monolayer of glutaraldehyde. To estimate the thickness of the different layers grafted on the silicon oxide modified surface, the attenuated intensity of Si2p peaks was considered according to the relation (1):

$$I = I_0 \exp(-d/\lambda \cos\theta) \quad (1)$$

where I_0 was the measured signal for SiO_2 electrons issued from the uncovered surface, I the signal measured for SiO_2 surface covered by an organic layer of thickness d, and λ the attenuation length of SiO_2 electrons in the organic layer, estimated within the range 20–30 Å (Powell and Jablonski, 2000). The layer thickness was estimated to be around 12-14 Å for APTES/glutaraldehyde, from the signal attenuation of the Si2p peak. This optimized functionalization process was then applied to modify SiNWs. SEM image of a modified nanowire is shown on Fig. 1-e, highlighting a glossy surface of the nanowire probably due to functionalization since it was not visible on unmodified SiNWs. The covalent immobilization of anti-LPS was then performed before adding *E. coli*. SEM images of interdigitated combs with nanowires and zoom on *E. coli* on nanowires is shown in Fig. 1. Typical size for *E.coli* were from 1 to 3 µm length range and nanowires had an average diameter of 100 nm with several micrometers in length.

3.2 Validation of bacteria immobilization using fluorescence analysis

Immobilization of bacteria on the nanowires was investigated by fluorescence analysis to confirm the binding. The dark image (Fig. 4a), reported after fluorescent analysis of functionalized silicon nanowires without bacteria and antibody free, confirmed that the surface did not contain any fluorescent element. In contrast, the immobilization of GFP bacteria on samples showed a significant difference of fluorescence signal intensity for two concentrations of bacteria: 10^6 CFU/mL and 10^8 CFU/mL (Fig. 4b and 4c). The image analysis allowed an estimate of the number of bacteria: 600 and 3387 respectively on square image (scale 200 µm). These fluorescence tests confirmed the validity of bacteria binding protocol on the modified surface of silicon nanowires for the anti-LPS/*E. coli* recognition.

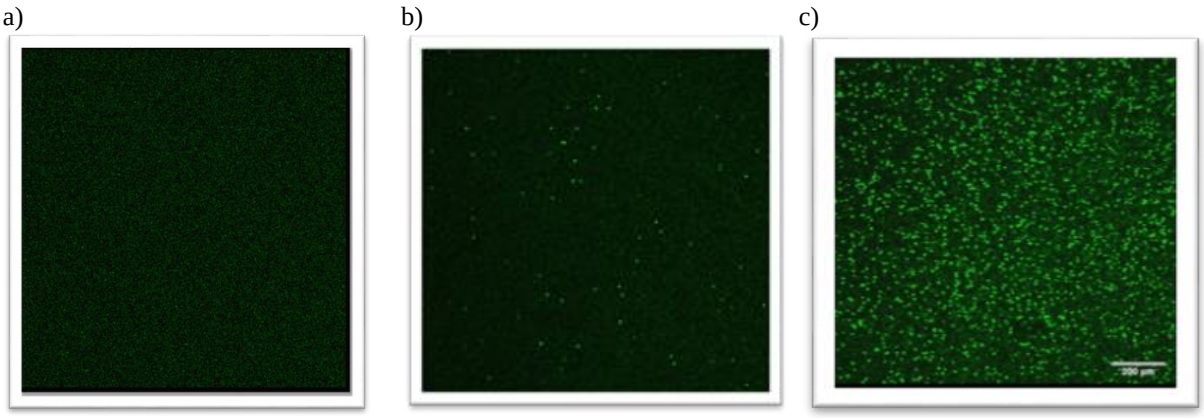

Figure 4: Fluorescence images of functionalized silicon nanowires a) without antibodies and bacteria as reference (blank), b) with antibodies and 10^6 CFU/mL *E. coli*, c) with antibodies and 10^8 CFU/mL *E. coli* (scale: 200 µm).

3.3 Electrical measurements before E. coli immobilization

At first, sensors were electrically characterized after the steps of chemical functionalization, antibodies immobilization and non-site-specific saturation on sensitive area made of SiNWs. The corresponding I (V) plot in Fig. 5a served as reference to control the binding of bacteria with antibodies. The curve is quasi-symmetrical with a non-ohmic behaviour at low voltages, as previously observed in a preliminary study with similar resistors for *E. coli* detection for yes/no diagnosis, for which no functionalization of silicon nanowires was performed (Le Borgne et al., 2018). This behaviour is related to the electrical model of the global electrical resistance (R_{tot}) of the resistor (Fig. 5b). Due to the symmetrical physical structure of the resistor R_{tot} can be written as $R_{tot} = V/I = 2xR_S + R_0/2n$, where n is the total number of interconnected teeth, R_S and R_0 represent the series and two adjacent teeths interconnected nanowires resistances, respectively. In this model, R_S is referred to the contact electrical resistance at the SiNW/N type polycrystalline silicon electrode interfaces. At low voltages, $R_0/2n$ dominates due to the high electrical resistivity of the undoped silicon nanowires array. In this case, energy barriers are induced at the interface between two interconnected SiNWs

(Pichon et al., 2015). For high voltages these energy barriers are lowered resulting to a decrease of R_0, and in this case the global electrical resistance is both controlled by the contributions of R_0 and R_S. Therefore, the domain of interest for bacteria detection was chosen for measurements at low voltages (-2V to 2V) where the nanowires electrical resistance dominated.

3.4 Electrical measurements after E. coli immobilization

Several dilutions with different concentrations 10^2-10^8 CFU/mL were then tested, and results are reported on Fig. 5c. After bacteria binding, an intensive rinsing was performed to remove the residues of the buffer solution and then the sensors were dried before the electrical measurements. The electrical measurements were performed in dry conditions to overcome the Debye length limitation due to the presence of other ions in solution. The electrical characteristic I(V) of the sensor shows no variation after buffer rinsing and drying as shown in Fig. S1. The value of the current level (Fig. 5c) raised with increasing bacteria concentrations. The current shift caused by bacteria was measured for several bias between 0 and 2 V and an optimised slope is observed for a voltage of 1.5V (Fig. 5d). The current level (measured at 1.5 V), increased linearly with the number of cells present in solution in the concentration range 10^2–10^8 CFU/mL, with a regression coefficient of 0.995. The estimated sensitivity, given by the slope of the current *versus* bacterial concentration characteristic, was 83 µA per decade of CFU/mL. This sensitivity remains interesting for the detection of pathogenic bacteria in most biological media. Bacterial culture thresholds beyond which an infection can be concluded are above this limit. For example: in the event of a urinary tract infection, the threshold is set at $<10^3$ CFU/mL, in the event of a pulmonary infection the significant threshold is between 10^2 and 10^5 CFU/mL depending on the types of samples.

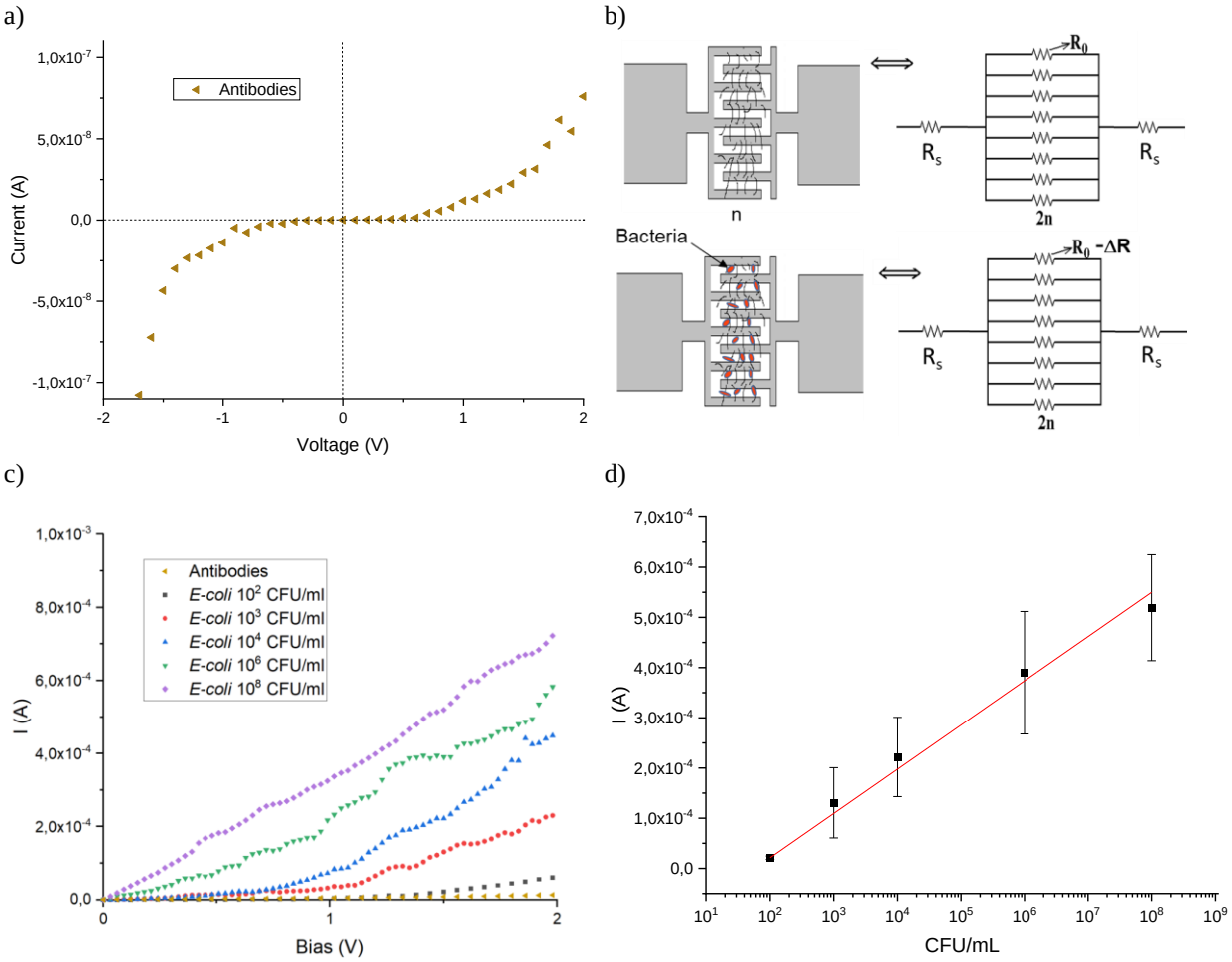

Figure 5: Electrical characteristic I (V), a) with antibodies, b) equivalent electrical model: the electrical résistance related to the SiNWs network varies after bacteria immobilization, c) with various concentration 10^2 to 10^8 CFU/mL *E. coli* bacteria on a single sensor or anti-LPS alone, and d) current shift versus bacterial concentration for a fixed 1.5 V bias, the slope of linear fit presents a regression coefficient of 0.995.

3.4 Specificity of the detection

We studied the specificity of electrical detection using *E. coli* anti-LPS antibodies, with Gram-negative (*E. coli*) and Gram-positive (*S. aureus)* strains. Two sensors were used and the nanowires were functionalized in the same way as those used previously. Thus, anti-LPS were attached to the surface, a blocking agent was applied to the sites between the silicon

nanowires, followed by the deposition of *S. aureus* (10^8 CFU/mL) and *E. coli* (10^8 CFU/mL) on each sensor (Fig. 6a). The SEM image in Fig. 6b showed round-shaped *S. aureus* with a diameter of about 1.5 µm. Fig. 6c showed the electrical response of the 2 sensors with anti-LPS functionalized nanowires, and after deposition of *S. aureus* and *E. coli* respectively (10^8 CFU/mL). *S. aureus* did not form a covalent bond with the antibody unlike the *E. coli* and thus, after washing and drying, the current was significantly higher on the sensor with *E. coli*. This confirms the elimination of non-specific bacteria after rinsing, thus demonstrating the specific detection of this system.

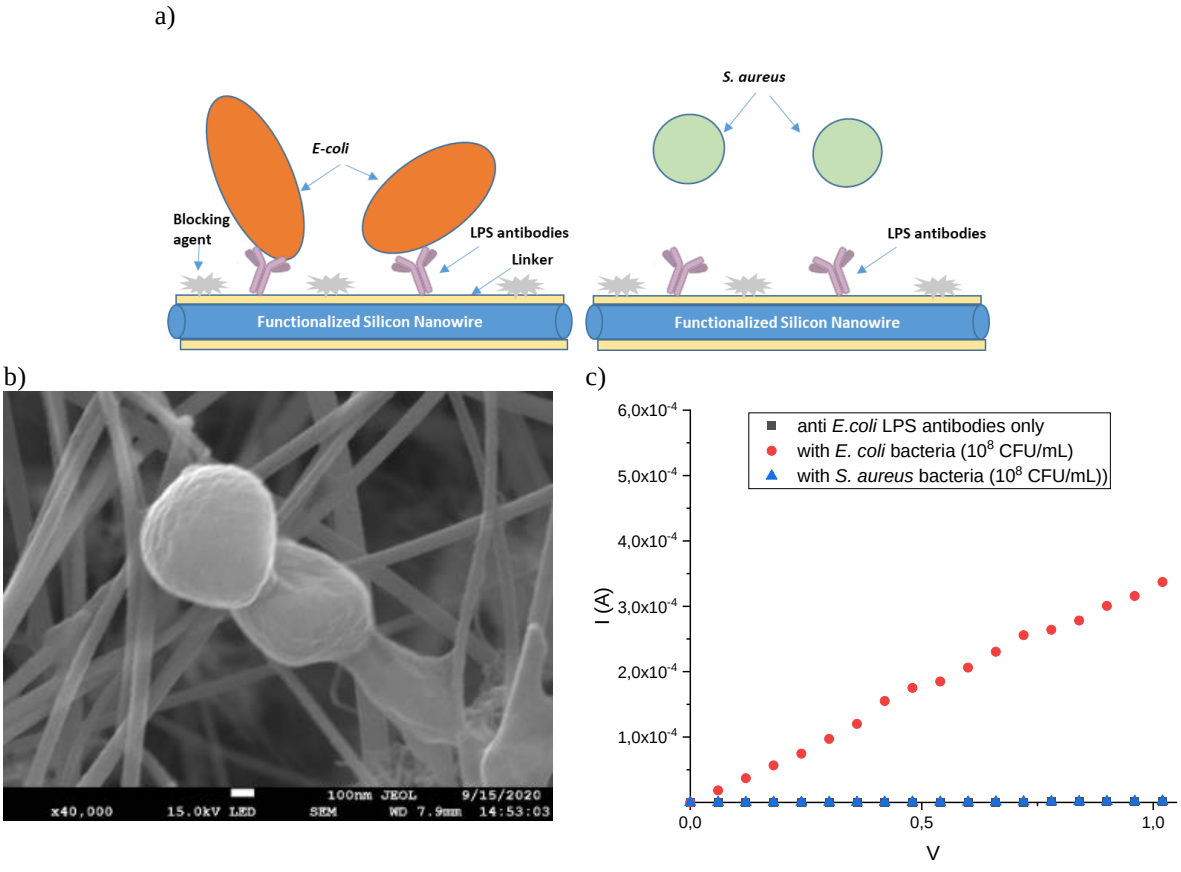

Figure 6: a) Schematic of the steps: functionalization, immobilization of antibodies, blocking agent and binding of bacteria (*E. coli* and *S. aureus*) on nanowires, then rinsing, b) SEM image of *S. aureus* bacteria on nanowires and c) electrical detection of *E. coli* and *S. aureus* bacteria (10^8 CFU/mL) using sensor with anti-LPS functionalized nanowires.

4. Discussion on the detection mechanism

The sensor developed in this study presents a very large number of interleaved and functionalized silicon nanowires facilitating the attachment of biomolecules and allowing an increased sensitivity to the detection of bacteria thanks to the nanometric dimensions of the nanowires and their high surface/volume ratio. A previous work (Lu et al., 2008) reported the electrical detection of *E. coli* using functionalized interdigited gold electrodes based sensors. In this work, only bacteria bridging the adjacent teeth of the electrodes are detected. In our sensor, numerous SEM observations have shown that bacteria preferentially cling to the functionalized nanowires and we did not observe bacteria on the silicon oxide surface located between the electrode teeth. The added values in using silicon nanowires network are: i) the three-dimensional configuration of the bacterial capture zone which offers an increased interaction surface between the sensitive part (the nanowire network) and all bacteria to be detected, and also ii) the possibility of field effect into the nanowires due to the electrical charge contained in the membrane of the bacteria acting as biological gate. These effects make it possible to expect an increased detection sensitivity compared to a sensor without nanowires. However, further study could be conducted to verify the benefit for using silicon nanowires in comparison with the direct use of bacteria to bridge electrodes reported in (Lu et al., 2008).

The sensor highlights specific detection of *E. coli*. The sensitivity we estimated with our sensor was 83 µA per decade of CFU/mL. This result is very promising for this type of biosensor for direct electrical detection at low levels of bacterial contamination (10^2 CFU/ml) required to ensure food safety (Huang et al., 2021)(Benserhir et al., 2022).

Several hypotheses could explain the increase of the current through the sensor after attachment of bacteria considering that: i) bacteria act as additional electrical conductive paths into the silicon nanowire array, ii) negative electrical charges of bacteria have a biochemical

gate effect allowing a change in electrical conduction of silicon nanowires by field effect, or iii) a possible transfer of electrical charges takes place into the nanowires. Silicon nanowire arrays have two major advantages: they have a significantly increased surface area compared to thin layers (high surface/volume ratio) and their conductance is very sensitive to their surface properties. Several conduction mechanisms are involved in conduction in SiNWs and the understanding of these mechanisms can be explained by several hypotheses, the main ones described by (Borowik et al., 2012) being Au-mediated surface conduction along the NW sidewalls and conduction through the SiNWs. In addition, this device can be adapted according to the needs, because it could be grafted with varied and modifiable specific antibodies according to the needs (airborne bacteria, targeted pathogenic bacteria, etc.). It is also transportable and could be used on different surfaces (clean rooms, operating rooms, etc.) or allow the detection of microorganisms in multiple environments.

With the presence of bacteria immobilized on the nanowires, conduction might be dominated by the electrical interaction between the nanowires and the membrane of *E. coli* cells. The outer membranes of Gram-negative bacteria are mainly composed of LPS molecules. Each LPS molecule has multiple negative electrical charges from phosphate and acid groups in the lipid A and core-polysaccharide (Adams et al., 2014). Since each bacterium carries negative electrical charges, the surface density of additional charges immobilized on the surface of the nanowires after bacteria attachment is then directly related to the measured current in the sensor. In their work, Susarrey-Arce *et al.* (Susarrey-Arce et al., 2016) have already investigated the interaction of *E. coli* with functionalized SiNWs surfaces. They explained that for Gram-negative *E. coli*, many adhesins are displayed on pili or fimbriae, which are hair-like appendages on bacterial cells that allow single cell to attach to surfaces. These extracellular structures and the rod-like shape of *E. coli* cells can generate multiple contact points with the irregular SiNWs arrays. Some authors have suggested that extracellular electron transport may be facilitated by extracellular conducting filaments, called bacterial

nanowires. Reguerra et al. indicated that the pili might serve as biological nanowires, transferring electrons from the bacterial cell surface to another surface (Reguera et al., 2005). El Naggar et al. demonstrated electrical transport along bacterial nanowires acting as a viable microbial strategy for extracellular electron transport (El-Naggar et al., 2010). These assumptions seem to be confirmed by the SEM image of *E. coli* (Fig. 1g) showing biological *pili* connecting the silicon nanowires. Then, the presence of bacterial nanowires and identification of the electron-transfer components that are required for electrical conductivity provide important advancements toward understanding the mechanisms involved in electron transfer. To demonstrate the concept of our system, we chose to test two very different bacterial types: Gram + cocci and Gram - bacilli, in order to be able to demonstrate that the electrical measurements carried out were possible, proportional to the quantity of bacteria, and specific considering the two species tested. This work is therefore a preliminary study to test the efficiency of the sensor.

4. Conclusions

The sensor developed in this study presents a very large number of interleaved and functionalized silicon nanowires facilitating the attachment of biomolecules and allowing the detection of bacteria thanks to the nanometric dimensions of the nanowires and their high surface/volume ratio. This work uses an approach that directly measures the contribution of bacteria, immobilized on the nanowires between two electrodes, by a significant current change. We thus demonstrated the feasibility of label-free detection for different concentrations of *E. coli*. The electrical measurements allowed the linear detection of bacterial concentrations in the range 10^2-10^8 CFU/mL with a high sensitivity of 83 µA per decade of CFU/mL and a specific detection. The results reported in this study show that the silicon nanowires-based resistor acts as a proof concept of sensor for direct and specific

detection of *E. coli* by electrical measurements. This SiNW biosensor device demonstrated its great potential as an alternative tool for future applications, as real-time bacterial detection with miniaturizable and low-cost electronic sensor for real time bacterial detection compatible with the classical silicon technology.

CRediT authorship contribution statement

Yousra Benserhir: Investigation, Resources, Formal analysis, Writing – original draft. Anne-Claire Salaün: Supervision, Investigation, Methodology, Formal analysis, Writing – original draft, Writing – review & editing, Funding Acquisition. Florence Geneste: Investigation, Methodology, Resources, Writing – review & editing. Nolwenn Oliviero: Investigation, Methodology. Laurent Pichon: Investigation, Formal analysis, Methodology, Writing – original draft, Writing – review & editing. Anne Jolivet-Gougeon: Investigation, Writing – review & editing, Validation.

Acknowledgments

This work was financial supported by University of Rennes 1. The authors thank the BIOSIT platform (University of Rennes1) for fluorescence imaging, Dr Aurélie Girard from IMN lab [Institut des Matériaux Jean Rouxel, University of Nantes) for XPS measurements and NANORENNES with IETR CNRS (UMR 6164) for SEM and EDS analysis.

References

Adams, P.G., Lamoureux, L., Swingle, K.L., Mukundan, H., Montaño, G.A., 2014. Lipopolysaccharide-Induced Dynamic Lipid Membrane Reorganization: Tubules, Perforations, and Stacks. Biophys. J. 106, 2395–2407. https://doi.org/10.1016/j.bpj.2014.04.016

Ahmed, A., Rushworth, J.V., Hirst, N.A., Millner, P.A., 2014. Biosensors for Whole-Cell Bacterial Detection. Clin. Microbiol. Rev. 27, 631–646. https://doi.org/10.1128/CMR.00120-13

Andrade, C.A.S., Nascimento, J.M., Oliveira, I.S., de Oliveira, C.V.J., de Melo, C.P., Franco, O.L., Oliveira, M.D.L., 2015. Nanostructured sensor based on carbon nanotubes and

clavanin A for bacterial detection. Colloids Surf. B Biointerfaces 135, 833–839. https://doi.org/10.1016/j.colsurfb.2015.03.037

Bao, L., Deng, L., Nie, L., Yao, S., Wei, W., 1996. Determination of microorganisms with a quartz crystal microbalance sensor. Anal. Chim. Acta 319, 97–101. https://doi.org/10.1016/0003-2670(95)00466-1

Benserhir, Y., Salaun, A.-C., Geneste, F., Pichon, L., Jolivet-Gougeon, A., 2022. Recent Developments for the Detection of Escherichia coli biosensors based on nano-objects – A review. IEEE Sens. J. 1–1. https://doi.org/10.1109/JSEN.2022.3160695

Borowik, Ł., Florea, I., Deresmes, D., Ersen, O., Hourlier, D., Mélin, T., 2012. Surface and Intrinsic Conduction Properties of Au-Catalyzed Si Nanowires. J. Phys. Chem. C 116, 6601–6607. https://doi.org/10.1021/jp300816e

Carvalho, F., Paradiso, P., Saramago, B., Ferraria, A.M., do Rego, A.M.B., Fernandes, P., 2016. An integrated approach for the detailed characterization of an immobilized enzyme. J. Mol. Catal. B Enzym. 125, 64–74. https://doi.org/10.1016/j.molcatb.2016.01.001

Chen, M.-C., Chen, H.-Y., Lin, C.-Y., Chien, C.-H., Hsieh, T.-F., Horng, J.-T., Qiu, J.-T., Huang, C.-C., Ho, C.-H., Yang, F.-L., 2012. A CMOS-Compatible Poly-Si Nanowire Device with Hybrid Sensor/Memory Characteristics for System-on-Chip Applications. Sensors 12, 3952–3963. https://doi.org/10.3390/s120403952

Cui, Y., 2001. Nanowire Nanosensors for Highly Sensitive and Selective Detection of Biological and Chemical Species. Science 293, 1289–1292. https://doi.org/10.1126/science.1062711

Dauphas, S., Ababou-Girard, S., Girard, A., Le Bihan, F., Mohammed-Brahim, T., Vié, V., Corlu, A., Guguen-Guillouzo, C., Lavastre, O., Geneste, F., 2009. Stepwise functionalization of SiNx surfaces for covalent immobilization of antibodies. Thin Solid Films 517, 6016–6022. https://doi.org/10.1016/j.tsf.2009.05.014

El-Naggar, M.Y., Wanger, G., Leung, K.M., Yuzvinsky, T.D., Southam, G., Yang, J., Lau, W.M., Nealson, K.H., Gorby, Y.A., 2010. Electrical transport along bacterial nanowires from Shewanella oneidensis MR-1. Proc. Natl. Acad. Sci. 107, 18127–18131. https://doi.org/10.1073/pnas.1004880107

Fasoli, A., Milne, W.I., 2012. Overview and status of bottom-up silicon nanowire electronics. Mater. Sci. Semicond. Process. 15, 601–614. https://doi.org/10.1016/j.mssp.2012.05.010

Gao, B., Rojas Chavez, A.A., Malkawi, W.I., Keefe, D.W., Smith, R., Haim, H., Salem, A.K., Toor, F., 2022. Sensitive detection of SARS-CoV-2 spike protein using vertically-oriented silicon nanowire array-based biosensor. Sens. Bio-Sens. Res. 36, 100487. https://doi.org/10.1016/j.sbsr.2022.100487

Gunda, N.S.K., Singh, M., Norman, L., Kaur, K., Mitra, S.K., 2014. Optimization and characterization of biomolecule immobilization on silicon substrates using (3-aminopropyl)triethoxysilane (APTES) and glutaraldehyde linker. Appl. Surf. Sci. 305, 522–530. https://doi.org/10.1016/j.apsusc.2014.03.130

Huang, T., Shi, Y., Zhang, J., Han, Q., Xia, X., Zhang, A.-M., Song, Y., 2021. Rapid and Simultaneous Detection of Five, Viable, Foodborne Pathogenic Bacteria by Photoinduced PMAxx-Coupled Multiplex PCR in Fresh Juice. Foodborne Pathog. Dis. 18, 640–646. https://doi.org/10.1089/fpd.2020.2909

Huang, Y., Dong, X., Liu, Y., Li, L.-J., Chen, P., 2011. Graphene-based biosensors for detection of bacteria and their metabolic activities. J. Mater. Chem. 21, 12358. https://doi.org/10.1039/c1jm11436k

Iucci, G., Battocchio, C., Dettin, M., Ghezzo, F., Polzonetti, G., 2010. An XPS study on the covalent immobilization of adhesion peptides on a glass surface. Solid State Sci. 12, 1861–1865. https://doi.org/10.1016/j.solidstatesciences.2010.01.021

Kaur, H., Shorie, M., Sharma, M., Ganguli, A.K., Sabherwal, P., 2017. Bridged Rebar Graphene functionalized aptasensor for pathogenic E. coli O78:K80:H11 detection. Biosens. Bioelectron. 98, 486–493. https://doi.org/10.1016/j.bios.2017.07.004

Kim, K., Park, C., Kwon, D., Kim, D., Meyyappan, M., Jeon, S., Lee, J.-S., 2016. Silicon nanowire biosensors for detection of cardiac troponin I (cTnI) with high sensitivity.

Biosens. Bioelectron. 77, 695–701. https://doi.org/10.1016/j.bios.2015.10.008

Le Borgne, B., Pichon, L., Salaun, A.C., Le Bihan, B., Jolivet-Gougeon, A., Martin, S., Rogel, R., de Sagazan, O., 2018. Bacteria electrical detection using 3D silicon nanowires based resistor. Sens. Actuators B Chem. 273, 1794–1799. https://doi.org/10.1016/j.snb.2018.07.101

Liao, W., Lin, Q., Xu, Y., Yang, E., Duan, Y., 2019. Preparation of Au@Ag core–shell nanoparticle decorated silicon nanowires for bacterial capture and sensing combined with laser induced breakdown spectroscopy and surface-enhanced Raman spectroscopy. Nanoscale 11, 5346–5354. https://doi.org/10.1039/C9NR00019D

Lu, Y.-C., Chuang, Y.-S., Chen, Y.-Y., Shu, A.-C., Hsu, H.-Y., Chang, H.-Y., Yew, T.-R., 2008. Bacteria detection utilizing electrical conductivity. Biosens. Bioelectron. 23, 1856–1861. https://doi.org/10.1016/j.bios.2008.03.005

Midahuen, R., Previtali, B., Fontelaye, C., Nonglaton, G., Stambouli, V., Barraud, S., 2022. Optimum functionalization of Si nanowire FET for electrical detection of DNA hybridization. IEEE J. Electron Devices Soc. 1–1. https://doi.org/10.1109/JEDS.2022.3166683

Mikolajick, T., Heinzig, A., Trommer, J., Pregl, S., Grube, M., Cuniberti, G., Weber, W.M., 2013. Silicon nanowires ‐ a versatile technology platform: Silicon nanowires ‐ a versatile technology platform. Phys. Status Solidi RRL ‐ Rapid Res. Lett. 7, 793–799. https://doi.org/10.1002/pssr.201307247

Ndieyira, J.W., Watari, M., Barrera, A.D., Zhou, D., Vögtli, M., Batchelor, M., Cooper, M.A., Strunz, T., Horton, M.A., Abell, C., Rayment, T., Aeppli, G., McKendry, R.A., 2008. Nanomechanical detection of antibiotic–mucopeptide binding in a model for superbug drug resistance. Nat. Nanotechnol. 3, 691–696. https://doi.org/10.1038/nnano.2008.275

Ni, L., Girard, A., Zhang, P., Jacques, E., Rogel, R., Salaun, A.C., Pichon, L., 2013. Au-Catalyst Silicon Nanowires Synthesized by Vapor–Liquid–Solid Technique in a V-Shaped Groove: Application for Gas Sensors. Sens. Lett. 11, 1541–1544. https://doi.org/10.1166/sl.2013.2842

Pichon, L., Rogel, R., Jacques, E., 2015. Electrical properties of phosphorus *in situ* doped Au-catalyst vapor liquid solid silicon nanowires. J. Appl. Phys. 118, 185701. https://doi.org/10.1063/1.4935278

Powell, C., Jablonski, A., 2000. NIST Electron Inelastic-Mean-Free-Path Database 71, Version 1.1. Nat'l Std. Ref. Data Series (NIST NSRDS) -, National Institute of Standards and Technology, Gaithersburg, MD.

Premasiri, W.R., Moir, D.T., Klempner, M.S., Krieger, N., Jones, G., Ziegler, L.D., 2005. Characterization of the Surface Enhanced Raman Scattering (SERS) of Bacteria. J. Phys. Chem. B 109, 312–320. https://doi.org/10.1021/jp040442n

Qin, Y., Cui, Z., Zhang, T., Liu, D., 2018. Polypyrrole shell (nanoparticles)-functionalized silicon nanowires array with enhanced NH3-sensing response. Sens. Actuators B Chem. 258, 246–254. https://doi.org/10.1016/j.snb.2017.11.089

Reguera, G., McCarthy, K.D., Mehta, T., Nicoll, J.S., Tuominen, M.T., Lovley, D.R., 2005. Extracellular electron transfer via microbial nanowires. Nature 435, 1098–1101. https://doi.org/10.1038/nature03661

So, H.-M., Park, D.-W., Jeon, E.-K., Kim, Y.-H., Kim, B.S., Lee, C.-K., Choi, S.Y., Kim, S.C., Chang, H., Lee, J.-O., 2008. Detection and Titer Estimation ofEscherichia coli Using Aptamer-Functionalized Single-Walled Carbon-Nanotube Field-Effect Transistors. Small 4, 197–201. https://doi.org/10.1002/smll.200700664

Susarrey-Arce, A., Sorzabal-Bellido, I., Oknianska, A., McBride, F., Beckett, A.J., Gardeniers, J.G.E., Raval, R., Tiggelaar, R.M., Diaz Fernandez, Y.A., 2016. Bacterial viability on chemically modified silicon nanowire arrays. J. Mater. Chem. B 4, 3104–3112. https://doi.org/10.1039/C6TB00460A

Thompson, M., Deisingh, A.K., 2004. Biosensors for the detection of bacteria. Can. J. Microbiol. 50.

Wang, P.W., Bater, S., Zhang, L.P., Ascherl, M., Craig, J.H., 1995. XPS investigation of electron beam effects on a trimethylsilane dosed Si(100) surface. Appl. Surf. Sci. 90,

413–417. https://doi.org/10.1016/0169-4332(95)00181-6
Yun, J., Ahn, J.-H., Moon, D.-I., Choi, Y.-K., Park, I., 2019. Joule-Heated and Suspended Silicon Nanowire Based Sensor for Low-Power and Stable Hydrogen Detection. ACS Appl. Mater. Interfaces 11, 42349–42357. https://doi.org/10.1021/acsami.9b15111
Zhang, X., Wang, D., Yang, D., Li, S., Shen, Z., 2012. Electronic Detection of Escherichia coli O157：H7 Using Single-Walled Carbon Nanotubes Field-Effect Transistor Biosensor. Engineering 04, 94–98. https://doi.org/10.4236/eng.2012.410B024